Autonomous Power Control in A Reconfigurable 6.78 Megahertz Multiple-receiver Wireless Charging System

He Yin, *Member, IEEE*, Minfan Fu, *Member, IEEE*, Ming Liu, *Member, IEEE*, Jibin Song, *Student Member, IEEE*, Chengbin Ma, *Member, IEEE*

Abstract—This paper proposes and implements autonomous control of a multiple-receiver wireless charging system. The charging control problem is challenging due to the decentralized nature of the system, possible changing numbers and types of energy storage devices as loads of the receivers, and complexity in wireless power distribution mechanism. The game theory-based control is developed that fully respects the unique characteristics of the transmitter (i.e., charger) and receivers. The preferences of the individual devices are first quantified using utility functions. Then the charging control problem is formulated as a generalized Stackelberg game considering the leader-follower relationship between the transmitter and receivers, and the limited total charging power. At each control instant, the generalized Nash equilibrium among the receivers, i.e., charging power distribution here, is reached by searching the Lagrange multiplier, while the total charging power from the transmitter is updated in a step-by-step manner. Both simulation and experimental results show that the proposed charging control autonomously manages and updates the power distribution in the cases where the receivers with different energy storage devices quit or join the wireless charging.

Index Terms—Autonomous charging control, game theory, generalized Stackelberg equilibrium, optimization, wireless power transfer.

I. INTRODUCTION

Due to the complementary features of energy storage devices (ESDs) such as different energy density and power density, it is natural to combine multiple types of ESDs (e.g., batteries, ultracapacitors, fuel cells, etc.) together that

H. Yin is with the Center for Ultra-Wide-Area Resilient Electric Energy Transmission Networks (CURENT), University of Tennessee, Knoxville, TN 37996, USA (e-mail: hyin8@utk.edu).

M. Fu is with the Center for Power Electronics Systems, Virginia Polytechnic Institute and State University, Blacksburg, VA 24061, USA (e-mail: minfanfu@vt.edu).

M. Liu is with Department of Electrical Engineering, Princeton University, Princeton, NJ 08544, USA (e-mail: ml45@princeton.edu).

J. Song and C. Ma are with the University of Michigan-Shanghai Jiao Tong University Joint Institute, Shanghai Jiao Tong University, Shanghai 200240, China (e-mail: jibinsong@sjtu.edu.cn; chbma@sjtu.edu.cn).

improves the overall performance, namely hybrid energy storage systems [1]. Such energy systems are actually a new type of networked systems, in which both information and power exchange among connected devices. It is interesting to note that similar to wireless communication, power can also be wirelessly delivered. This new possibility could further improve the flexibility of power distribution in networked energy systems, particularly reconfigurable ones. Now near-field wireless power transfer (WPT) is popular such as through the inductive resonance coupling, which works either at kilohertz (kHz) or several megahertz (MHz) [2]. In terms of spatial freedom, namely longer transfer distance and higher tolerance to coil misalignment, increasing the operating frequency to MHz is usually desirable because it enables transferring of the same amount of power (i.e., efficient operation) but with weaker coupling between the transmitting coil and receiving coil. This advantage is especially important to build a flexible WPT system that can simultaneously charge multiple receiving devices such as wearable devices and cell phones. In real applications, the receiving devices may have quite different size, position, and orientation that in turn require a high degree of spatial freedom of the WPT. In addition, a higher operating frequency results in a more compact and lighter WPT system. Meanwhile, a major limitation lies in the performance of present power electronic devices at MHz. Thus the MHz WPT is now widely considered to be suitable for mid-range and low-power applications such as charging of various consumer electronic devices [2].

Based on the above considerations, this paper discusses the modeling and control of a multiple-receiver wireless charging system working at 6.78 MHz, the lowest center frequency at MHz in ISM (industrial, scientific, and medical) band [3]. The 6.78 MHz is now widely considered to be cost effective for low-power applications. In the system, multiple types of energy storage devices such as different batteries are wirelessly and simultaneously charged sharing the same transmitter, i.e., charger. For this less common multiple-receiver WPT system, most of existing research so far is on its analysis and modeling aspects such as circuit models, the coupling effect among receiving coils and its compensation, and impedance matching [4], [5]. It is known that multiple devices can be wirelessly charged with different resonant frequencies, namely multifrequency WPT [6], [7]. A drawback of the multifrequency WPT is that it cannot enable simultaneous charging of the receiving devices. The narrow ISM bands also limit its

actual application. As to the knowledge of the authors, there is a lack of work on control strategies and their implementation that actively manage the power distribution inside a multiple-receiver WPT system. This task is challenging due to the complexity in the mechanism of the wirelessly transferred power and decentralized nature of the system. In real applications the numbers and types of the receiving devices may change over time. This further adds difficulty in the power distribution control. Synergy, flexibility, and scalability are required when discussing a proper control strategy for the multiple-receiver wireless charging system. In order to fully respect the unique characteristics of the receivers and transmitter, game theory-based control is proposed. Thanks to its decentralized nature, the proposed approach helps to achieve autonomy in the power distribution control, particularly when the charging system is reconfigured.

Game theory is now well-known to be a powerful tool to represent interactions among self-interested players and predict their choices of strategies [8]. This aspect is especially useful to autonomously update the strategy when a system is reconfigured. Game theory-based control has been recently applied in power electronic systems and power systems. In [9], the control decision problem in small-scale and dc power systems is represented as a game between players that facilitates the definition of individual sources and loads. [10] develops game-theoretic-based modeling for bus selection in multibus dc power systems, which is based on local information of the player and thus eliminates the need of a centralized controller. [11] applies a game-theoretic approach in the path optimization of load players during a cold start in a small-scale power system. [12] studies a game theory-based load sharing strategy that maximizes the overall efficiency of a system consisting of multiple power electronic converters in parallel. In this paper, the mechanism for implementing the power distribution control is first explained using the circuit model of a general multiple-receiver WPT system. Because the transmitter is a "leader" that determines the total available charging power, the solution of the game theory-based control is a generalized Stackelberg equilibrium [13], [14]. At this equilibrium, the receivers negotiate and jointly determine their shared portions of the total charging power (i.e., generalized Nash equilibrium), and the transmitter tries to minimize its output power in a step-by-step manner. For reference purposes, a centralized optimization-based control is also developed using the same utility functions and constraints. It shows that unlike the optimization-based control, the game theory-based one does not require specific local information of the individual devices, just the corresponding decisions, as particularly discussed in section V-B. This advantage enables the autonomous power distribution when the receivers with different types of batteries quit or join the wireless charging (i.e., enhanced flexibility and scalability). Finally, the theoretical discussions are validated through simulation and experiments using an example three-receiver wireless charging system.

II. POWER DISTRIBUTION MECHANISM

The circuit model of a general n-receiver WPT system is shown in Fig. 1, where L, C, and R with different subscripts
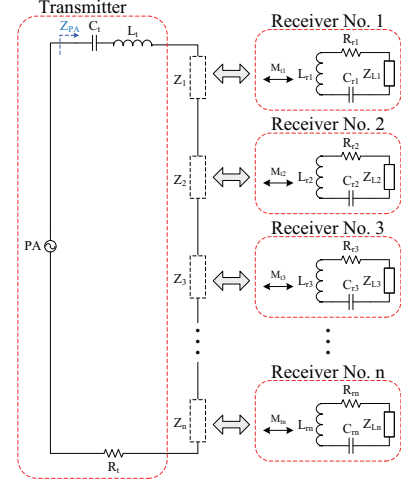

Fig. 1. Equivalent circuit model of a general n-receiver wireless charging system.

$(t, r_1, r_2, r_3, \text{ or } r_n)$ represent the coil inductance, compensation capacitance, and parasitic resistance of a corresponding coil. Under resonance, the following relationships exist,

$$j\omega L_k + \frac{1}{j\omega C_k} = 0 \text{ for } k = t, r_1, r_2, \ldots, r_n. \quad (1)$$

Assuming that there are no overlaps among the receivers, the cross coupling among the coils is usually neglectable [5], [15]. Thus the reflected impedance Z_i, i.e., the loading effect of the ith receiver on the transmitter, can be derived as [15],

$$Z_i = \frac{\omega^2 M_{ti}^2}{R_{ri} + Z_{Li}} \text{ for } i = 1, 2, \ldots, n, \quad (2)$$

where ω is the operating frequency, 6.78 MHz here; M_{ti} is the mutual inductance between the transmitting coil and the ith receiving coil; Z_{Li} is the equivalent load impedance seen by the receiving coil.

Again, as shown in (1), under the resonance, Z_{pa}, the load impedance seen by the power amplifier (PA), is

$$Z_{pa} = R_t + \sum_{i=1}^{n} Z_i. \quad (3)$$

The output power from the PA, p_{pa}, is first transferred to the ith receiving coil, and then to the load Z_{Li}. Thus the power received by Z_{Li} is

$$p_{Li} = p_{pa} \frac{Re\{Z_i\}}{R_t + \sum_{i=1}^{n} Re\{Z_i\}} \frac{Re\{Z_{Li}\}}{R_{ri} + Re\{Z_{Li}\}}. \quad (4)$$

$Re\{*\}$ means the real part of a complex number and R_{ri} is the parasitic resistance of the ith receiving coil. Since R_{ri} is usually much smaller than $Re\{Z_{Li}\}$ (e.g., 0.65 Ω versus 20–30 Ω in the following final experiments), then

$$p_{Li} \approx p_{pa} \frac{Re\{Z_i\}}{R_t + \sum_{i=1}^{n} Re\{Z_i\}}, \quad (5)$$

and

$$p_{L1} : p_{L2} : \cdots : p_{Ln} = Re\{Z_1\} : Re\{Z_2\} : \cdots : Re\{Z_n\}. \quad (6)$$

Based on (6), the power distribution among the receivers is determined by Z_i's, actually Z_{Li}'s, the load impedances seen by the receiving coils [refer to (2)].

In order to control Z_{Li}'s (i.e., the power distribution), dc-dc converters can be added between the rectifiers and final loads (ESDs here) [2]. For a dc-dc converter such as a buck converter used in this paper, its input resistance R_{dcdc} seen by the rectifier is known to equal

$$R_{dcdc} = \frac{R_L}{D^2}, \qquad (7)$$

where D is the duty cycle of the single switch inside the buck converter, and R_L is the actual final load [see Fig 2.]. The controllable R_{dcdc} through the power-width-modulation (PWM) control of the converter determines the value of a Z_{Li} and thus the power distribution among the receivers, as shown in the above two equations, (6)(7). Physically the duty cycles of the dc-dc converters can be determined through PI (Proportional-Integral)-based control. In the present multiple-receiver wireless charging system, the final loads connecting with the dc-dc converters are battery cells. The game theory-based control developed below works to determine a proper reference distribution of the battery charging powers in an autonomous manner, which is implemented through the PWM control of the dc-dc converters in the following experiments.
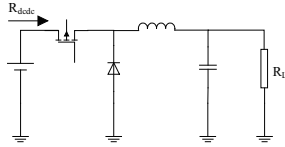

Fig. 2. Buck converter.

Note that the relationship among the reflected impedances, Z_i's in Fig. 1, is independent with a specific compensation topology of the transmitting coil. In addition, the final purpose of the above PWM-based control of the dc-dc converter is to actively adjust the value of Z_i that already includes the influence of M_{ti}, the mutual inductance [refer to (2)]. The above mechanism of charging power distribution and adjustment is a general conclusion and thus implementable for other different compensation topologies (e.g., parallel-series (PS), series-parallel (SP), and parallel-parallel (PP) topologies) including the LC parallel or LLC compensation in the transmitting side. It also works in the cases where there are changed mutual inductances due to variations in coil relative positions (e.g., distances, alignments, and orientations).

III. DEFINITION OF UTILITY FUNCTION

A. Receivers

In a multiple-receiver wireless charging system, there are one transmitter and n receivers. In order to achieve the autonomous control of the power distribution, they are modeled as independent players. Two different types of the players exist in the system, leader and follower. The player of the transmitter is a leader that determines the total available charging power, p_{total}, while the players of the receivers are the followers that compete on the limited charging power, namely

$$\sum_{i=1}^{n} p_i \leq p_{total}, \qquad (8)$$

where p_i is the distributed charging power to the ESD, i.e., the final load, in the i-th receiver. Note that physically all the p_i's here are greater than zero, and they have one-to-one relationship with p_{Li}'s in (6).

The preferences of the receivers, i,e., their utility functions u_i, and their weight coefficients w_i can be defined as follows,

$$u_i = \ln(p_i + 1) \text{ and } w_i = \frac{P_i^*}{SOC_i}. \qquad (9)$$

SOC_i is the state of charge (SOC) of the ESD in the i-th receiver and P_i^* is the preferred charging power of the ESD such as a recommended value from the data sheet of a specific battery. Equation (9) is chosen as the utility function of the receivers due to the following reasons:

1) The logarithmic functions have been widely used for modeling the demand preference of users [16].
2) When the distributed charging power p_i is zero, u_i equals zero. On the other hand, the improvement rate in u_i, i.e., $\frac{1}{p_i+1}$, is the largest when $p_i = 0$. This rate decreases with an increasing p_i, and eventually becomes very small when p_i is unnecessarily large.
3) The relative importance of the preference of a specific receiver is represented by w_i. It is proportional to the desired battery charging power, P_i^*, and inversely proportional to the SOC of the battery.

For the protection of battery, here the range of the distributed charging power is limited as follows,

$$0 \leq p_i \leq P_i^*. \qquad (10)$$

B. Transmitter

For the leader, the transmitter, its utility function, i.e., preference, is defined as

$$u_t = \ln\left[e - (e - 1)\frac{p_{total}}{P_{max}}\right], \qquad (11)$$

where e is the base of the mathematical constant and P_{max} is the maximum permissible charging power provided by the transmitter. As same as in (9), a logarithmic function is chosen to represent the preference of the transmitter, namely minimizing its output power. Its utility function, u_t, is maximized when p_{total} is simply zero, while u_t becomes zero when p_{total} reaches the maximum permissible power, P_{max}. Note that at the same time, a constraint on p_{total} must be first satisfied,

$$\sum_{i=1}^{n} p_i \leq p_{total} \leq P_{max}. \qquad (12)$$

Thus the transmitter may have to increase its output power if needed, namely compromising its preference to meet the constraint on required total charging power. Practically, p_{total} can be controlled by regulating the PA dc supply voltagpe, v_{pa}. Again p_i's, namely the charging power distribution, are determined by performing the duty-cycle control of the dc-dc converters in the receivers, i.e., adjusting the equivalent load resistances seen by the rectifiers.

IV. Optimization based Control

For reference purposes, a classical centralized optimization is first developed. It is assumed that all the necessary global and local information from both transmitter and receivers is available to a centralized controller, namely p_{total}, n, p_i ($i = 1, \cdots, n$), P_{max}, P_i^*, SOC$_i$. Besides, changes in the number and type of the receivers are supposed to be exactly known. Thus the solution of each of those possible cases can be preciously solved. Note that the above assumptions make the centralized control less flexible when facing a reconfigurable wireless charging system, in which the involved receivers may dynamically quit or join the charging system.

Due to the leader-follower relationship, a two-stage optimization is performed to solve the charging power distribution among the receivers. At the first stage of the optimization, the utility functions of the receivers are used as objective functions (OBJs),

$$\text{OBJ}_1 : f_{min} = -u_1, \ \cdots, \ \text{OBJ}_n : f_{min} = -u_n, \quad (13)$$

subject to

$$\sum_{i=1}^{n} p_i \leq p_{total}. \quad (14)$$

In order to achieve an analytical solution instead of a numerical or heuristic one, the final objective function is formulated as follows,

$$\text{OBJ} : f_{min} = -\sum_{i=1}^{n} w_i u_i, \quad (15)$$

where w_i's are the weights previously defined in (9). This nonlinear optimization problem can be solved using the well-known Karush-Kuhn-Tucker (KKT) conditions [17]. Equations (14) and (15) are first formed into the Lagrangian function L,

$$L = -\sum_{i=1}^{n} w_i \ln(p_i + 1) + v\left(\sum_{i=1}^{n} p_i - p_{total}\right). \quad (16)$$

Let

$$\frac{\partial L}{\partial p_i} = -\frac{w_i}{p_i + 1} + v = 0, \text{ for } i = 1, \ldots, n \quad (17)$$

$$\frac{\partial L}{\partial v} = \sum_{i=1}^{n} p_i - p_{total} = 0, \quad (18)$$

then the candidate KKT point can be solved as,

$$p_i = \frac{w_i(p_{total} + n) - \sum_{i=1}^{n} w_i}{\sum_{i=1}^{n} w_i}, \text{ for } v = \frac{w_i}{p_i + 1} \quad (19)$$

$$p_i = P_i^*, \text{ for } v = 0. \quad (20)$$

Due to the convexity, the Hessian of the Lagrangian function is always positive definite. Therefore, (19) or (20) is a global optimal point. As discussed above in section II, the calculated p_i's are physically achieved through the duty-cycle control of the dc-dc converters in the receivers.

At the second stage of the optimization, again the utility function of the transmitter is directly used as the objective function,

$$\text{OBJ}_t : f_{min} = -u_t, \quad (21)$$

subject to the constraint on the total available charging power, p_{total}, in (12). For the second stage optimization, since (21) is a monotonous function, the solution always exists on the boundary box, i.e., $\sum_{i=1}^{n} p_i$ and P_{max}. Given the solution from the first stage optimization, the $\sum_{i=1}^{n} p_i$ will be either $\sum_{i=1}^{n} P_i^*$ or P_{max}, namely

$$p_{total} = min\left(\sum_{i=1}^{n} P_i^*, P_{max}\right). \quad (22)$$

In the following final experiments, the control of p_{total} is implemented through PA dc supply voltage (v_{pa}) regulation.

V. Game Theory based Control

In real applications, there could be unpredictable and changing number of the individual receivers. The types and the characteristics of their included ESDs may also be quite different. The flexibility of power delivery by WPT makes it convenient to charge such reconfigurable energy storage systems. However, this new possibility prefers a control strategy that can autonomously perform the power distribution control in a dynamic environment. Here, besides the optimization-based centralized control, an alternative solution, the game theory-based control, is developed below, in which the transmitter and receivers are modeled and treated as independent players. This aspect well matches the decentralized nature of the present charging control problem. Similarly, the distributed charging power (p_i) and total available charging power (p_{total}) are experimentally achieved through the dc-dc converter duty cycle control and PA dc supply voltage regulation, respectively.

A. Generalized Stackelberg Game

The preferences of the players, i.e., the transmitter and receivers, have been discussed in section III. Using the same utility functions, the charing control problem is treated here as a so-called generalized Stackelberg game [14], [18]. In this game, the followers (i.e., receivers) determine their respective charging power under the limitation of the total available charging power, p_{total}, at the last control instant. Then the leader (i.e., transmitter) updates p_{total} according to the decisions of the followers, p_i's, namely the feedback information from the followers. The game continues, in which the leader and followers make their decisions by turns, namely a so-called two-stage game [19]. For the followers, they are considered to be "selfish" and non-cooperative. They negotiate on the distribution of charging power among themselves. The leader is also "selfish" reducing its output power as much as possible. Meanwhile, as a supplier of charging power, it is required to satisfy the power requirements from the receivers. Due to the constraint on the total available charging power in (8), the final solution is a generalized Stackelberg equilibrium. In this solution, the receivers reach the generalized Nash equilibrium instead of the classical Nash equilibrium and the transmitter minimizes its output power. The Nash equilibriums are common solutions in game theory to solve non-cooperative games [20]. Under the generalized Stackelberg equilibrium, no device, either the transmitter or receivers, has incentive to alter its present decision.

1) Generalized Nash equilibrium among receivers: Under the constraint on the total available charging power, (8), each follower's (a receiver here) admissible strategy set depends on the other followers' decisions, i.e., the generalized Nash equilibrium problem in a static noncooperative game [21] [22]. First the existence of the generalized Nash equilibrium (GNE) is mathematically proved below using the KKT conditions. For a specific receiver, its utility function, u_i, and the constraint in (8) can be combined to form the Lagrangian function L_i,

$$L_i(p_i, \lambda_i) = u_i + \lambda_i G(p_i, \overline{\mathbf{p}}_{-\mathbf{i}}), \tag{23}$$

where

$$G(p_i, \overline{\mathbf{p}}_{-\mathbf{i}}) = \sum_{i=1}^{n} p_i - p_{total}, \tag{24}$$

λ_i is the Lagrange multiplier, and $\overline{\mathbf{p}}_{-\mathbf{i}}$ is the vector formed by all the followers' decision variables, i.e., the distributed charging power here, except the one of the ith follower.

Since (9) is concave, the KKT conditions are the necessary and sufficient conditions for the proof of the existence the GNE. The KKT conditions of the i-th follower's optimization problem are

$$\frac{\partial L_i}{\partial P_i} = -\frac{w_i}{p_i + 1} + \lambda_i = 0, \tag{25}$$

$$G(p_i, \overline{\mathbf{p}}_{-\mathbf{i}}) \leq 0, \tag{26}$$

and it is known that the KKT conditions are satisfied with [14], [23]

$$\lambda_1 := \lambda_2 := ... := \lambda_n := \overline{\lambda}. \tag{27}$$

Note that if (27) holds, the GNE is the most socially stable one [14]. When $\overline{\lambda} = 0$, i.e., $p_{total} > \sum_{i=1}^{n} p_i$, it is straightforward that

$$p_i = P_i^* \text{ for } \overline{\lambda} = 0. \tag{28}$$

Thus the charging power of each ESD is rightly at its preferred value. Otherwise, combining (25) and (27) gives the solution for non-zero $\overline{\lambda}$, i.e., a balanced decision on competing the total available power p_{total} among the followers,

$$p_i = \frac{w_i(p_{total} + n)}{\sum_{i=1}^{n} w_i} - 1 \text{ for } \overline{\lambda} \neq 0. \tag{29}$$

Thus the existence of the GNE is proved. Again, since all the u_i's in (9) are concave, the above solution of p_i's is unique.

Unlike in (29), in real implementation the GNE is reached by searching $\overline{\lambda}$ when the receivers need to compete on the limited total available charging power p_{total}, as shown in the flow chart, Fig. 3. A local leader is chosen from the receivers to broadcast $\overline{\lambda}$. Note that this local leader does not gain any extra benefit. Thus it can be randomly selected such as the receiver No. 1 in this paper [24]. For convenience purposes, the initial values of p_i ($i = 1, \ldots, n$) and $\overline{\lambda}$ are P_i^* and zero, respectively. If p_{total} is sufficient (i.e., $\sum p_i < p_{total}$), it is natural that all ESDs in the receivers are simply charged by their respective preferred charging powers, P_i^*'s. Note that, for searching $\overline{\lambda}$, the initial values of p_i can also be other proper values that help to improve the convergence speed. This aspect is further discussed in the following experiments in

section VI-E. From (25), $\overline{\lambda}$ is always positive. Thus a positive and small perturbation $\Delta\overline{\lambda}_k$ is applied

$$\Delta\overline{\lambda}_k = K_p \left(\sum_{i=1}^{n} p_i - p_{total} \right), \tag{30}$$

in a step-by-step manner in order to locate the GNE. The coefficient, K_p, determines the convergence speed of $\overline{\lambda}$. After each perturbation, the constraint, (8), is evaluated. If the constraint is violated, the perturbation needs to be updated and applied again in the following step. This procedure is iteratively repeated until the constraint is met. Based on the above mathematical proof, it is guaranteed that there is only one single $\overline{\lambda}$ satisfying the constraint. Thus from (25), p_i's, i.e., the GNE, can be calculated as

$$p_i = \frac{w_i}{\overline{\lambda}} - 1. \tag{31}$$

Different with the proof in (29), p_i is determined by its own weight coefficient w_i and iteratively searched $\overline{\lambda}$. Note that w_i contains the local information of the i-th receiver, namely P_i^* and SOC_i [refer to (9)], and the value of $\overline{\lambda}$ is based on the exchange of decisions of all the receivers, i.e., p_i's, as shown in (30) and Fig. 3.
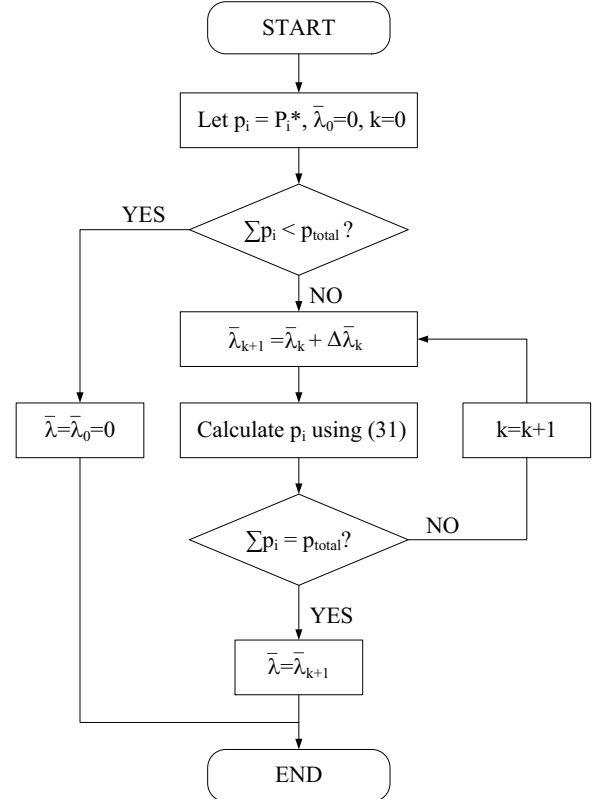

Fig. 3. Flowchart for the procedure of searching the Lagrange multiplier.

2) Total power optimization: In the present game, due to the constraint in (8), the receivers need to seek GNE instead of the classical Nash equilibrium. Thus the game is a generalized Stackelberg equilibrium problem, and its solution is the so-called generalized Stackelberg equilibrium (GSE) [14], [25]. From (11)(12), the utility function and the constraint of the

transmitter, the optimal p_{total} from the transmitter can be simply solved as

$$p_{total} = min\left(\sum_{i=1}^{n} p_i + \Delta P, P_{max}\right), \qquad (32)$$

namely, maximized efficiency (i.e., minimized P_{total}) for a specific combination of receivers. Again, p_{total} is determined by its local information, P_{max}, and the decisions of all the receivers. Note $\sum_{i=1}^{n} p_i$ varies with the different number of the receivers, n, and the types and SOCs of the included ESDs. Due to the nature of this Stackelberg leader-follower game, the change of n is supposed to be unpredictable. And for the transmitter, the leader, the characteristics of the individual ESDs in the receivers are also unknown. Thus a small positive ΔP is added in (32), which provides the transmitter a capability to update the newest p_{total} in a step-by-step manner. Besides, considering various losses in a real WPT system, practically ΔP also serves as a safe margin to provide sufficient charging power through having a slightly larger PA dc supply voltage, v_{pa}. Note that ΔP is a user defined parameter, which is 0.2 W in the following simulation and experiments. As shown in Fig. 4, the GSE is reached at every control instant using the algorithm discussed above [refer to the flowchart in Fig. 3 and (32)]. Here T is the control period.
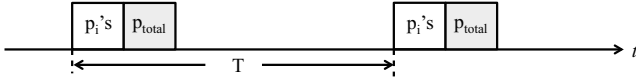

Fig. 4. Time sequence for solving GSE.

TABLE I
COMPARISON ON SHARED INFORMATION.

Control	Global information	Local information
Optimization-based	p_{total}, p_i, n	P_{max}, P_i^*, SOC_i
Game theory-based	$p_{total}, p_i, \overline{\lambda}$	(none)

B. Autonomy in Charging Power Distribution

As discussed above, the game theory-based approach is partly based on the KKT conditions. It is expected that the results using the game theory-based control would converge to those under the optimization-based one. An obvious difference between the two approaches is the requirement on the shared information, as summarized in Table I. When applying the optimization-based control, in order to determine the charging power distribution, the centralized controller needs to collect all the global (p_{total}, p_i, n) and local information (P_{max}, P_i^*, SOC_i). This requirement also leads to reformulation of the control problem particularly there are receivers dynamically join or quit the charging (i.e., a changing n). On the contrary, in the game theory-based control, only p_{total}, p_i, and $\overline{\lambda}$ are shared among the local controllers in the transmitter and receivers (see Fig. 3). Note that $\overline{\lambda}$ is broadcasted only among receivers. All the local information, P_{max} in the transmitter, and P_i^* and SOC_i in the receivers, is well preserved within an individual device. The exchange of local formation is not

required in the game theory-based control. This advantage can potentially improve the flexibility and scalability of the charging power distribution in a dynamic environment such as with dynamically changing number of individual receivers.

For instance, when there is a new receiver joining the wireless charge, the conventional optimization-based control needs to recollect all the global and local information including the newest number of receivers, the preferred charging power (P_i^*) and the ESD's SOC of the newly added receiver. The centralized controller then updates the objective function and constraints again, and calculates the supplied power and its distribution among the receivers. As a decentralized solution, in the game theory-based control, the new receiver only needs to share its decision, i.e., a specific p_i, under the same $\overline{\lambda}$ among all the receivers. Its internal characteristics, i.e., the local information P_i^* and SOC_i, are not required by the other local controllers. Because the decision making in a specific device only depends on its local information, the game theory-based control enables autonomous power distribution, i.e., the solution represented by the GSE, when the multiple-receiver wireless charging system is reconfigured. This aspect is verified and further explained below through simulation and experiments.
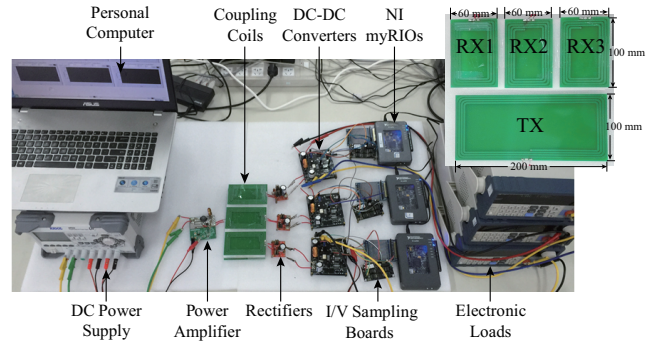
VI. SIMULATION AND EXPERIMENTAL RESULTS

Fig. 5. Experimental multiple-receiver wireless charging system.

A. Experimental System

Fig. 5 shows a multiple-receiver wireless charging system built up for the following experiments, in which a single transmitting coil (TX) is placed below n ($n \leq 3$) receiving coils (RXs) with a vertical distance of 20 mm. Both TX (100×200 mm) and RXs (60×100 mm) are four-turn coils. The trace width and trace spacing of the coils are 2.5 mm and 0.8 mm, respectively. TX and RXs are aligned to have a mutual inductance coefficient of 0.15. The positions of RXs are fixed and above TX. The measured cross coupling coefficient between RXs is about 0.005, which is neglectable comparing with the mutual inductance coefficient between TX and RXs. The charging power is transferred from the transmitting coil to the receiving coils through inductive resonance coupling working at 6.78 MHz. Again, the improved spatial freedom via a higher operating frequency makes the MHz WPT particulary suitable for charging multiple consumer electronics devices
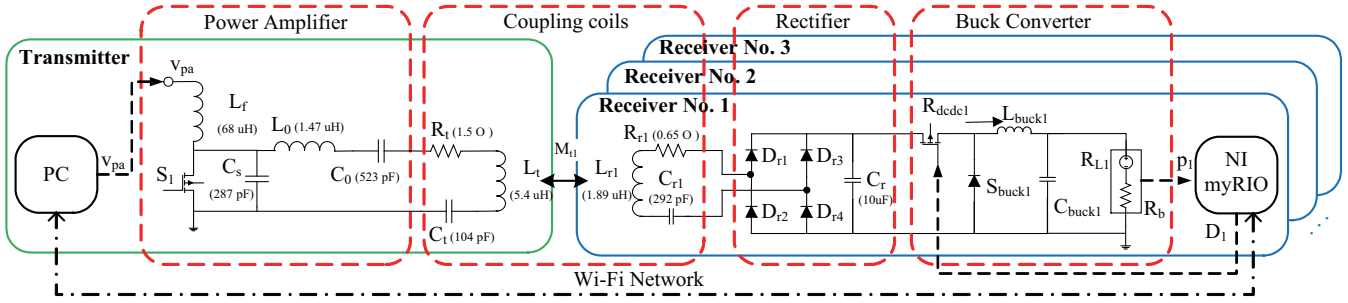
Fig. 6. Schematic diagram of the experimental multiple-receiver wireless charging system.

such as wearable devices and cell phones. At the same time, as discussed above, the proposed autonomous power control itself is a general approach that can be applied to other multiple-receiver WPT systems with different operating frequencies, power levels, and configurations.

As shown in Fig. 5 and the schematic diagram in Fig. 6, in the transmitter the Class E power amplifier (PA) inverts dc power into 6.78 MHz ac power and drives the transmitting coil, while the received ac power is converted back to dc power through the rectifier, a full-bridge one [26]. The connected dc-dc converter is the charging management circuit. In the following experiments, the average efficiencies of the rectifiers and dc-dc converters are 91% and 89%, respectively. For convenience, the electronic loads are programmed to emulate the dynamic behaviors of the ESDs, different types of lithium-ion batteries here, based on the well-known equivalent circuit models of batteries [27]. Note that the equivalent loads seen by the rectifiers, R_{dcdc1}−R_{dcdc3} in Fig. 6, are actively controlled by the buck converters. Thus the power distribution mechanism discussed in section II is still valid when the final loads are battery cells.

In order to implement the decentralized autonomous charging control, the controllers for transmitter and receivers should be physically independent ones. Considering this requirement, three National Instruments (NI) myRIOs are used as the controllers for the receivers, while the transmitter is controlled by a personal computer (PC). These four controllers communicate with each other through a Wi-Fi network, namely a unique charging system in which both power and information are wirelessly connected. Note that the frequency ranges of a Wi-Fi signal are in GHz bands. Thus there is no interference between the Wi-Fi communication system and wireless charging system. The PC provides the PA reference dc supply voltage signal, v_{pa}^*, to the dc power supply through universal serial bus (USB) connection, and thus determines the total charging power available to the receivers, i.e., p_{total}, following the experimentally-calibrated relationship between v_{pa} and p_{total} (details are omitted to conserve space). The PC also controls the electronic loads to run the dynamic battery models via RS232 serial communication ports. For each receiver, the NI myRIO samples the voltage and current of its load, i.e., an ESD here, and calculates the duty cycle, D, of the dc-dc converter that eventually decides the charging power distribution among the receivers.

The initial PA input dc voltage, v_{pa}, is 25 V, and it varies

TABLE II
PARAMETERS OF EXPERIMENTAL SYSTEM.

[Transmitter]				
PA MOSFET	C_t	L_t	R_t	v_{pa}
SUD15N15	104 pF	5.40 μH	1.50 Ω	15–30 V
[Receivers]				
Rec. Diode	C_{ri}	L_{ri}	R_{ri}	
STPSC406	292 pF	1.89 μH	0.65 Ω	
[Batteries]				
Cell	Capacity	Voltage	Resistance	Mass
Lishen	12.5 Ah	3.2 V	8 mΩ	370 g
Sanyo	2.5 Ah	3.7 V	100 mΩ	48 g

between 15–30 V. The key parameters of the transmitter, receivers, and battery cells are further summarized in Table II [refer to Fig. 1]. Two types of lithium-ion battery cells are emulated by the electronic loads, 12.5-Ah Lishen LP2770102AC LiFePO$_4$ cell and 2.5-Ah Sanyo 18650 LiCoO$_2$ cell, using their respective dynamic models [27]. These two cells are selected to represent the cases in which the charged ESDs have very different characteristics and requirement on the desired charging power and current. The Lishen cell is a battery for traction purposes, whose $\frac{C}{3}$ is five times larger than that of the Sanyo cell (i.e., 12.5 Ah and 2.5 Ah.). The initial SOCs, SOC_{ini}, of the cells in No. 1–3 receivers are assumed to be 30%, 50%, and 70%, respectively, in all the following three cases. Case A emulates quitting of the wireless charging, in which all the three ESDs are with same type, Sanyo cells, while in Cases B and C different types of ESDs (Lishen or Sanyo cells) quit and join the charging. The cases are designed to emulate random cases and thus verify the performances of the game theory- and optimization-based controls when managing the charging power distribution in a reconfigured multiple-receiver wireless charging system.

In the below three cases, the GSE and optimization-based solution are both updated in every two seconds, i.e., $T= 2$ s [refer to Fig. 4]. This relatively long control period is due to the slow response time of the dc power supply in the present experimental setup. K_p and ΔP are taken as 0.01 and 0.2 W, respectively, via trial-and-error tuning. Note that these two parameters should be specified based on the required convergence speed and accuracy in a target application.

B. Case 1: Quitting Charging-Same ESDs

In this case, the ESDs in the three receivers are all Sanyo 2.5-Ah cells. As shown in Fig. 7, the No. 3 and 2 receivers

quit the wireless charging at 30 and 60 s, respectively. This case is designed to verify the control when the maximum charging power from the transmitter is sufficient to supply the desired charging power of all the ESDs in the receivers, i.e., a $\frac{C}{3}$ (≈ 0.83 A) charging current for each cell here. Before quitting, each receiver is charged at its desired power P_i^* ($i = 1, 2, 3$) that corresponds to the $\frac{C}{3}$ current. Thus $\overline{\lambda}$ is simply zero and the GNE settled at $p_i = P_i^*$ [refer to (28)]. The total charging power, p_{total}, from the transmitter is also minimized accordingly. The oscillations in the experimental power responses show the transients of the decentralized charging control in the real implementation. Due to the pre-assumed unpredictable quitting of a specific receiver, the excessive power is first distributed to the other receivers, which explains the overshoots in the responses, while the nonlinear behavior of the PA causes the undershoots when updating v_{pa}, the PA input dc voltage, for a lower total charging power.

The basic trend of the experimental results (exp.) well matches that of the simulation results (sim.) for both game theory-based and optimization-based control. This verifies the theoretical correctness of the proposed charging control and its implementation. Note that for a theoretical verification, in simulation the PI-based duty-cycle control of the dc-dc converter is not included. p_i's and p_{total} are directly given after the calculation. In this case, since there is no need for searching $\overline{\lambda}$, the simulated or theoretical performances of the game theory- (GT) and optimization-based (Opt) controls are identical.
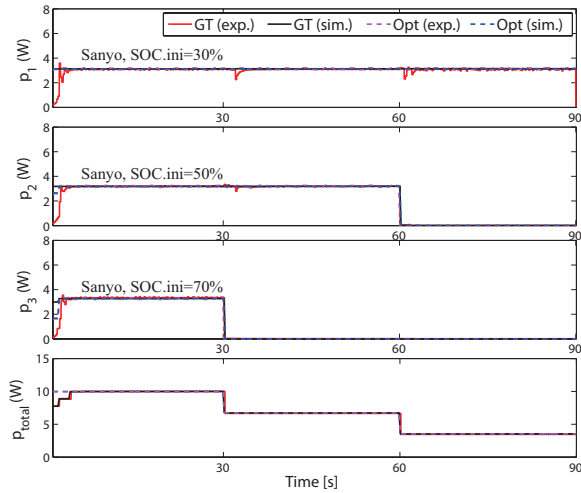

Fig. 7. Power distribution and total charging power in case 1.

C. Case 2: Quitting Charging-Different ESDs

Here the ESDs in No. 1 and 2 receivers are still the 2.5-Ah Sanyo cells, while the cell in No. 3 is the Lishen 12.5-Ah one, a cell requiring much larger charging current and preferred charging power P_3^* (again, corresponding to its own $\frac{C}{3}$ current). Note that cases 2 and 3 are designed to verify the proposed control when the receivers require very different charging power. Again the No. 3 and No. 2 receivers quit at 30 and 60 s, respectively. As shown in Fig. 8, different

with the results in case 1, the three receivers can not achieve their respective preferred charging power anymore due to the limited total charging power from the transmitter. The devices, the three receivers and transmitter, have to jointly determine a balanced power distribution, i.e., a GSE, in a step-by-step manner. As same as the expectation, the results through the game theory-based control converge to those under the optimization-based one taking 11 iterations. With both global and local information available, the optimization-based control directly gives the optimal solution. However, as discussed above, its centralized nature sacrifices control flexibility in a dynamic environment, particularly when the number of the receivers varies. Thus the advantage of applying the game theory-based control is not to outpace the classical optimization-based control in the final control performance, but to enable autonomy in charging power distribution [refer to section V-B]. Note that after the No. 3 receiver quits the charging after 30 s, the results become same with those in Case 1 because the power capability of the transmitter is sufficient to charge the left two receivers with their preferred charging power, namely P_1^* and P_2^*.
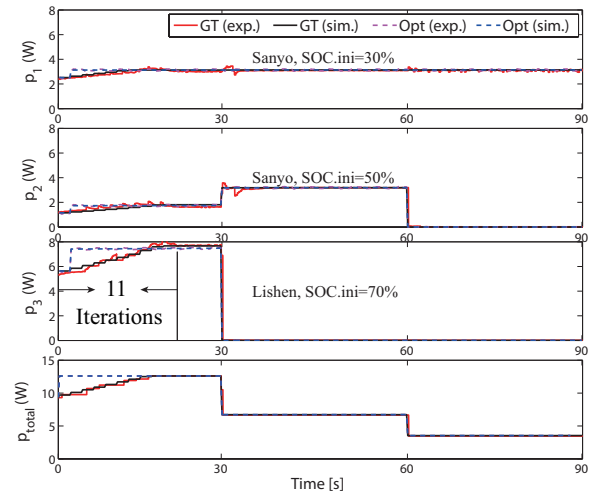

Fig. 8. Power distribution and total charging power in case 2.

D. Case 3: Joining Charging-Different ESDs

In this case, initially there is only one receiver, the No. 1 receiver, whose ESD is the Sanyo 2.5-Ah cell. At 30 s, the No. 2 receiver joins the charging with an ESD of a Sanyo 2.5-Ah cell too. Next at 60 s, No. 3 receiver also joins the charging, but its ESD is the Lishen 12.5-Ah cell, the one with a much higher capacity. Again, under the game theory-based control, the first two receivers eventually settle at a GNE in which the receivers are charged with their preferred charging power, P_1^* and P_2^*, respectively. After the joining of the No. 3 receiver, which requires a much larger charging power, a new GNE is reached in which the charging powers of the No. 1 and 2 receivers deviate from their original preferred ones. The new GNE settles at the one as same as the first GNE reached in Case 2.
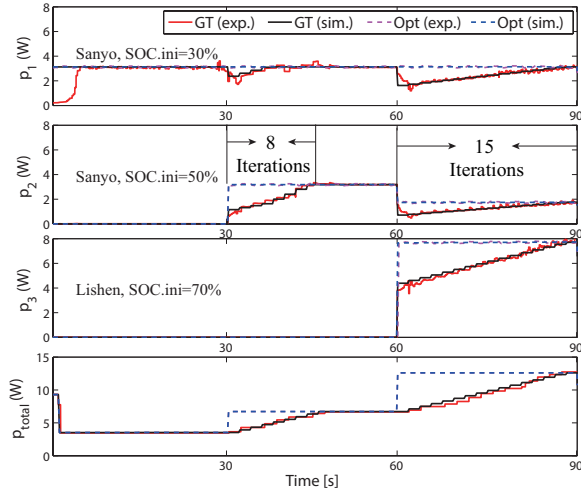
Fig. 9. Power distribution and total charging power in case 3.

TABLE III
CHARGING POWER DISTRIBUTION IN CASE 3.

Receiver	$SOC_{ini,i}$	P_i^*	30 s	60 s	90 s
No. 1-Sanyo	30%	3.08 W	3.11 W	3.09 W	3.10 W
No. 2-Sanyo	50%	3.08 W	–	3.20 W	1.91 W
No. 3-Lishen	70%	13.33 W	–	–	7.75 W

E. Additional Discussions

The average dc-dc system efficiencies (i.e., from the dc power supplier to electronic loads), η_{avg}, for the game theory-based control in the three cases are 52.7%, 52.0%, and 52.4%, respectively. The average efficiencies for the optimization-based control are 54.1%, 53.9% and 54.2%, respectively. Again, the game theory-based control yields comparable efficiencies to the centralized optimization-based control, but with obviously enhanced flexibility and scalability. The efficiencies could be further enhanced through the efforts on the hardware aspect such as improved design of rectifiers and dc-dc converters. Meanwhile, due to the nature of the present multi-objective optimization and control problem, there is always tradeoff between desired charging power distribution and the overall system efficiency.

The charging power distribution well reflects the defined utility functions, i.e., the preferences, in section III and the tradeoff relationship among the receivers and transmitter. As shown in Table III taking case 3 as an example, at 30 s the No. 1 cell is charged by 3.11 W, namely its preferred charging power, P_1^*=3.08 W; when the No. 2 cell joins the wireless charging, it is charged by the preferred charging power too because the total available charging power from the transmitter is sufficient; while when the No. 3 cell, which requires much larger charging power, joins the charging after 60 s, the charging power is autonomously redistributed thanks to the mechanism proposed in section II and game theory-based control. Due to the low SOC, the No. 1 cell is still charged by its preferred charging power, while the No. 2 and 3 cells are charged with 62.01% and 58.14% of their respective preferred charging power due to the differences in the capacity and SOC of the two battery cells.

The required iterations when searching $\overline{\lambda}$, the Lagrange multiplier, are investigated taking different initial values of p_i, not necessarily P_i^*. As an example, in the below Fig. 10, a wide range (0–10 times of P_1^*) of the initial value of p_1 can be taken that does not significantly increase the required number of iterations to reach the GNE among the receivers. It is natural that the iterations, which is reversely proportional to the convergence speed, decrease when the initial value of p_1 is close to P_1^*, 3.08 W here.
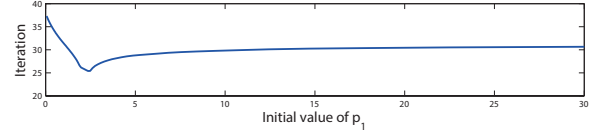

Fig. 10. An example of the average required iterations over the entire duration (0–90 seconds) when searching $\overline{\lambda}$ in case 3 (P_1^*=3.08 W).

The flexibility and scalability of the game theory-based control is quantitatively studied assuming the number of receivers varies between 1 and 50. A 10000-case Monte Carlo analysis is performed for each number of receivers. The parameters (SOC$_i$: 0.3–0.7; P_i^*: 3–8 W) are uniformly distributed within their respective ranges. As shown in Fig. 11, the minimum, maximum, and average numbers of required iterations versus the number of receivers follow logarithmic trend lines instead of exponential ones. This result further verifies the enhanced flexibility and scalability through the game theory-based control when dealing with the cases with a changing number of receivers. It also shows the computational efficiency of the control particularly with a large number of receivers.
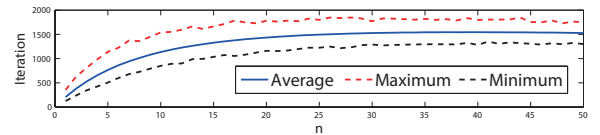

Fig. 11. A 10000-case Monte Carlo analysis under different numbers of receivers (1–50).

Fig. 12 and Table IV further show the performance comparison of four possible control methods in experiments, spontaneous control (i.e., passive control), SOC-based control, optimization-based control, and game theory-based control. In the spontaneous control, the dc-dc converters simply operate with a fixed duty cycle that maximizes each reflected impedance Z_i [refer to (2) and (7)]. Thus the power received by a single receiver could be possibly maximized. However, as shown in (6), in a multi-receiver WPT system the power distribution is actually determined by the ratio among Z_i's. Meanwhile, in the SOC-based control, the charging power is distributed reversely proportional to the SOCs of the ESDs in the receivers. In the both above controls, v_{pa} is maximized to be able to provide sufficient charging power. As shown in Fig. 12, the power distribution under the passive spontaneous control is uncontrollable; the SOC-based control also shows poor performance especially within the last 30 seconds (60–90 seconds) when the transmitter can not provide the total

required charging power from all the three receivers. This is because the Lishen 12.5-Ah cell in the No. 3 receiver has a higher initial SOC (70%), but it requires a much larger charging power due to its higher capacity than those of the other two Sanyo 2.5-Ah cells. In Table IV, two criteria, the average dc-dc system efficiency η_{avg} and average ratio of p_i to P_i^*, in case 3 are applied for comparison purposes. It is obvious the game theory-based control shows much better performance than those of the spontaneous control and SOC-based control. Again, the game theory-based control has comparable performance to that of the ideal optimization-based control, but with obviously improved flexibility and scalability, as shown and discussed in the above sections.

The proposed game theory-based control requires a local controller for each receiver and a relatively complicated algorithm. At the same time, it enables autonomy in the charing power distribution. This unique advantage makes the game theory-based control particularly suitable to deal with the control of complicated energy systems such as the multiple-receiver wireless charing system in which the receivers join and quite charging unpredictably. Besides, the computational efficiency of the distributed approaches such as the game theory-based control also helps to lower the computational cost especially when the number of the devices is large.
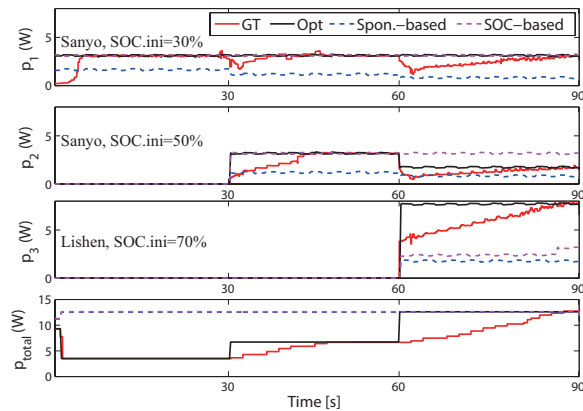

Fig. 12. Power distribution and total charging power in case 3 under the game theory-based control, optimization-based control, spontaneous control, and SOC-based control.

TABLE IV
CONTROL PERFORMANCE COMPARISON IN CASE 3.

Spec.	Spontaneous control	SOC-based control	Optimization-based control	Game theory-based control
η_{ave} (%)	15.9%	34.4%	54.2%	52.4%
$Ave(\frac{p_1}{P_1^*})$	0.32	0.97	0.97	0.88
$Ave(\frac{p_2}{P_2^*})$	0.39	0.95	0.74	0.57
$Ave(\frac{p_3}{P_3^*})$	0.13	0.16	0.52	0.42

VII. CONCLUSIONS

This paper proposes and experimentally implements a game theory-based autonomous power control of a less common multiple-receiver wireless charging system. Due to the flexibility provided by the WPT, different numbers and types

of the ESDs can be simultaneously charged as the loads of the receivers. However, the complex characteristics and the decentralized nature of the system make the charging control challenging. The possibly reconfigured system configuration further complicates the discussion on the control and its implementation. In order to achieve autonomy in the power control, the decentralized game theory-based control is proposed and developed that fully respects the performance and requirements of each individual device. The solution of the charging control is a generalized Stackelberg equilibrium, in which only the global information is required. The charging power distribution is determined and updated through the negotiation among the present receivers, namely a generalized Nash equilibrium. Thus the charging control is flexible to handle the cases where the numbers and types of charged ESDs change over time, as verified both in the simulation and the final experiments. The future work may include extending the approach to more complex wireless or conventional networked energy systems and further exploring the improvements in flexibility, scalability, and reliability of the energy management.

REFERENCES

[1] H. Yin, C. Zhao, M. Li, and C. Ma, "Utility function-based real-time control of a battery ultracapacitor hybrid energy system," *IEEE Trans. Ind. Informat.*, vol. 11, no. 1, pp. 220–231, Feb., 2015.

[2] M. Fu, C. Ma, and X. Zhu, "A cascaded boost–buck converter for high-efficiency wireless power transfer systems," *IEEE Trans. Ind. Informat.*, vol. 10, no. 3, pp. 1972–1980, Aug., 2014.

[3] "Improving the effectiveness, flexibility and availability of spectrum for short range devices," in *Document RAG07-1/17-E, , Radiocommunication Advisory Group, International Telecommunication Union*, Jan., 2007.

[4] J. Kim, D.-H. Kim, and Y.-J. Park, "Analysis of capacitive impedance matching networks for simultaneous wireless power transfer to multiple devices," *IEEE Trans. Ind. Electron.*, vol. 62, no. 5, pp. 2807–2813, May, 2015.

[5] M. Fu, T. Zhang, X. Zhu, P. Luk, and C. Ma, "Compensation of cross coupling in multiple-receiver wireless power transfer systems," *IEEE Trans. Ind. Informat.*, vol. 12, no. 2, pp. 474–482, Apr., 2016.

[6] Z. Pantic, K. Lee, and S. M. Lukic, "Receivers for multifrequency wireless power transfer: Design for minimum interference," *IEEE J. Emerg. Sel. Topics Power Electron.*, vol. 3, no. 1, pp. 234–241, Mar., 2015.

[7] D. Ahn and P. P. Mercier, "Wireless power transfer with concurrent 200-khz and 6.78-mhz operation in a single-transmitter device," *IEEE Trans. Ind. Electron.*, vol. 31, no. 7, pp. 5018–5029, Jul., 2016.

[8] E. Stephens, D. Smith, and A. Mahanti, "Game theoretic model predictive control for distributed energy demand-side management," *IEEE Trans. Smart Grid*, vol. 6, no. 3, pp. 1394–1402, May, 2015.

[9] W. W. Weaver and P. T. Krein, "Game-theoretic control of small-scale power systems," *IEEE Trans. Power Del.*, vol. 24, no. 3, pp. 1560–1567, May, 2009.

[10] N. C. Ekneligoda and W. W. Weaver, "A game theoretic bus selection method for loads in multibus dc power systems," *IEEE Trans. Ind. Electron.*, vol. 61, no. 4, pp. 1669–1678, Apr., 2014.

[11] ——, "Game-theoretic cold-start transient optimization in dc microgrids," *IEEE Trans. Ind. Electron.*, vol. 61, no. 12, pp. 6681–6690, Dec., 2014.

[12] P. Bartal and I. Nagy, "Game theoretic approach for achieving optimum overall efficiency in dc/dc converters," *IEEE Trans. Ind. Electron.*, vol. 61, no. 7, pp. 3202–3209, Jul., 2014.

[13] R. B. Myerson, *Game theory*. Harvard university press, 2013.

[14] W. Tushar, W. Saad, H. Poor, and D. Smith, "Economics of electric vehicle charging: A game theoretic approach," *IEEE Trans. Smart Grid*, vol. 3, no. 4, pp. 1767–1778, Dec., 2012.

[15] M. Fu, T. Zhang, C. Ma, and X. Zhu, "Efficiency and optimal loads analysis for multiple-receiver wireless power transfer systems," *IEEE Trans. Microw. Theory Tech.*, vol. 63, no. 3, pp. 801–812, Mar., 2015.

[16] W. Tushar, B. Chai, C. Yuen, D. B. Smith, K. L. Wood, Z. Yang, and H. V. Poor, "Three-party energy management with distributed energy resources in smart grid," *IEEE Trans. Ind. Electron.*, vol. 62, no. 4, pp. 2487–2498, Apr., 2015.

[17] N. Rahbari-Asr and M.-Y. Chow, "Cooperative distributed demand management for community charging of phev/pevs based on kkt conditions and consensus networks," *IEEE Trans. Ind. Informat.*, vol. 10, no. 3, pp. 1907–1916, Aug., 2014.

[18] A. Belgana, B. Rimal, and M. Maier, "Open energy market strategies in microgrids: A Stackelberg game approach based on a hybrid multiobjective evolutionary algorithm," *IEEE Trans. Smart Grid*, vol. 6, no. 3, pp. 1243–1252, May, 2015.

[19] Z. Zhou, J. Bai, M. Dong, K. Ota, and S. Zhou, "Game-theoretical energy management design for smart cyber-physical power systems," *Cyber-Physical Systems*, vol. 1, no. 1, pp. 24–45, Feb., 2015.

[20] T. Basar and G. J. Olsder, *Dynamic noncooperative game theory*. SIAM, 1999, vol. 23.

[21] F. Facchinei and C. Kanzow, "Generalized Nash equilibrium problems," *Annals of Operations Research*, vol. 175, no. 1, pp. 177–211, Mar., 2010.

[22] W. Saad, Z. Han, H. V. Poor, and T. Basar, "Game-theoretic methods for the smart grid: An overview of microgrid systems, demand-side management, and smart grid communications," *IEEE Signal Processing Magazine*, vol. 29, no. 5, pp. 86–105, Sep., 2012.

[23] A. A. Kulkarni and U. V. Shanbhag, "On the variational equilibrium as a refinement of the generalized Nash equilibrium," *Automatica*, vol. 48, no. 1, pp. 45–55, Jan., 2012.

[24] Z. Zhang and M.-Y. Chow, "Convergence analysis of the incremental cost consensus algorithm under different communication network topologies in a smart grid," *IEEE Trans. Power Syst.*, vol. 27, no. 4, pp. 1761–1768, Nov., 2012.

[25] G. Leitmann, "On generalized stackelberg strategies," *Journal of Optimization Theory and Applications*, vol. 26, no. 4, pp. 637–643, Dec., 1978.

[26] M. Fu, H. Yin, M. Liu, and C. Ma, "Loading and power control for a high-efficiency Class E PA-Driven megahertz WPT system," *IEEE Trans. Ind. Electron.*, vol. 63, no. 11, pp. 6867–6876, Nov., 2016.

[27] R. C. Kroeze and P. T. Krein, "Electrical battery model for use in dynamic electric vehicle simulations," in *IEEE Power Electronics Specialists Conference (PESC'08)*, Rhodes, Greece, Jun., 2008, pp. 1336–1342.

Ming Liu (S'15-M'17) received the B.S. degree from SiChuan University, Sichuan, China, in 2007, and the M.S. degree from the University of Science and Technology Beijing, Beijing, China, in 2011, both in mechatronic engineering, and the Ph.D. degree in electrical and computer engineering at University of Michigan-Shanghai Jiao Tong University Joint Institute, Shanghai Jiao Tong University, Shanghai, China, in 2017.

He is currently a postdoctoral research fellow at Department of Electrical Engineering, Princeton University, Princeton, NJ, USA. Between 2012 and 2014, he was an assistant research fellow with Shenyang Institute of Automation, Chinese Academy of Sciences, Shenyang, China. His research interests include high frequency resonant converters, wireless power transfer systems, power electronics and applications, circuit-level and system-level optimization.

Jibin Song (S'16) received the B.S. degree in measurement & control technology and instrumentation from Jilin University, Jilin, China, in 2016. He is currently working toward the Ph.D. degree in electrical and computer engineering, University of Michigan-Shanghai Jiao Tong University Joint Institute, Shanghai Jiao Tong University, Shanghai, China. His research interests include general power electronics, design and optimization of multiple-receiver megahertz wireless power transfer systems.

He Yin (S'13-M'16) received the B.S. and Ph.D. degree in the electrical and computer engineering from University of Michigan-Shanghai Jiao Tong University Joint Institute, Shanghai Jiao Tong University, Shanghai, China in 2012 and 2017, respectively.

He is currently a postdoctoral researcher at Center for Ultra-Wide-Area Resilient Electric Energy Transmission Networks (CURENT), University of Tennessee, Knoxville, TN, USA. His research interests include optimization and energy management of microgrids and wireless power transfer systems, and phasor measurement unit (PMU) design.

Chengbin Ma (M'05) received the B.S. (Hons.) degree in industrial automation from the East China University of Science and Technology, Shanghai, China, in 1997, and the M.S. and Ph.D. degrees both in electrical engineering from the University of Tokyo, Tokyo, Japan, in 2001 and 2004, respectively.

He is currently an Associate Professor of electrical and computer engineering at University of Michigan-Shanghai Jiao Tong University Joint Institute, Shanghai Jiao Tong University, Shanghai, China. Between 2006 and 2008, he held a postdoctoral position with the Department of Mechanical and Aeronautical Engineering, University of California Davis, California, USA. From 2004 to 2006, he was an R&D researcher with Servo Laboratory, Fanuc Limited, Yamanashi, Japan. He is an Associate Editor of the IEEE Transactions on Industrial Informatics. His research interests include energy management, megahertz wireless power transfer, dynamics and motion control, and wide applications in electronic devices, electric vehicles, microgrids and smart grids, etc.

Minfan Fu (S'13-M'16) received the B.S., M.S., and Ph.D. degrees in electrical and computer engineering from University of Michigan-Shanghai Jiao Tong University Joint Institute, Shanghai Jiao Tong University, Shanghai, China in 2010, 2013, and 2016, respectively.
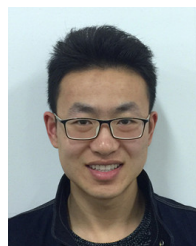
He is currently a postdoctoral researcher at the Center for Power Electronics Systems, Virginia Polytechnic Institute and State University, Blacksburg, VA, USA. His research interests include megahertz wireless power transfer, high-frequency power conversion, high-frequency magnetic design, and applications of wide-band-gap devices.